ACS APPLIED MATERIALS & INTERFACES

Research Article

www.acsami.org

Fast Switching Water Processable Electrochromic Polymers

Pengjie Shi,[†] Chad M. Amb,[†] Aubrey L. Dyer,[†,‡] and John R. Reynolds*[,†,‡]

[‡]School of Chemistry and Biochemistry, and School of Materials Science and Engineering, Center for Organic Photonics and Electronics, Georgia Institute of Technology, Atlanta, Georgia 30332, United States

[†]The George and Josephine Butler Polymer Research Laboratory, Department of Chemistry, Center for Macromolecular Science and Engineering, University of Florida, Gainesville, Florida 32611, United States

Supporting Information

ABSTRACT: This paper describes the synthesis of two new blue to transmissive donor−acceptor electrochromic polymers: a polymer synthesized using an alternating copolymerization route (ECP-Blue-A) and a polymer synthesized using a random copolymerization (ECP-Blue-R) by Stille polymerization. These polymers utilize side chains with four ester groups per donor moiety, allowing organic solubility in the ester form, and water solubility upon saponification to their carboxylate salt form. We demonstrate that the saponified polymer salts of ECP-Blue-A and ECP-Blue-R (WS-ECP-Blue-A and WS-ECP-Blue-R) can be processed from aqueous solutions into thin films by spray-casting. Upon the subsequent neutralization of the thin films, the resulting polymer acid films are solvent resistant and can be electrochemically switched between their colored state and a transmissive state in a KNO_3/water electrolyte solution. The polymer acids, WS-ECP-Blue-A-acid and WS-ECP-Blue-R-acid, show electrochromic contrast $\Delta\%T$ of 38% at 655 nm and 39% at 555 nm for a 0.5 s switch, demonstrating the advantage of an aqueous compatible electrochrome switchable in high ionic conductivity aqueous electrolytes. The results of the electrochromic properties study indicate that these polymers are promising candidates for aqueous processable and aqueous switching electrochromic materials and devices as desired for applications where environmental impact is of importance.

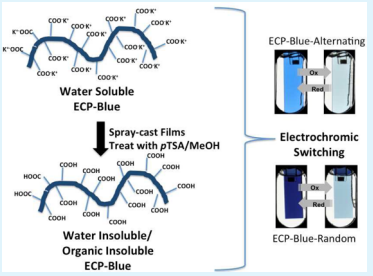

KEYWORDS: *electrochromism, water-soluble electroactive polymers, Stille polymerization*

INTRODUCTION

The utilization of π-conjugated polymers is significantly influenced by their optoelectronic properties as well as their solution processability. In this regard, fine-tuning of desired properties by synthetic modification of the polymer backbone and nature of the pendant groups is perhaps the most widely used tool.[1] Despite there being a large number of conjugated polymers with diverse material properties, which have been synthesized and evaluated for applications such as OLEDs,[2−4] OPVs,[5−7] FETs,[8,9] and ECDs,[10−13] only a handful of materials have demonstrated widespread commercial success such as poly(3-hexylthiophene), poly(2-methoxy-5-(2-ethylhexyloxy)-1,4-phenylenevinylene) (MEH-PPV) and poly(3,4-ethylenedioxythiophene): poly(styrene sulfonate) (PEDOT:PSS). Of those listed, PEDOT:PSS has made the largest impact across a wide variety of applications from capacitors, to hole transport layers, antistatic coatings, and electrochromics. This is largely due to its highly processable nature, which affords it the ability to be processed from an aqueous solution yielding thin films with a high conductivity.[14,15] In addition, the high contrast between a deep blue neutral state and a highly transmissive oxidized state makes PEDOT:PSS a strong candidate for electrochromic applications.[16−18] The combination of aqueous processability, similar to that of PEDOT:PSS, with the color tunability of other electrochromic polymer (ECP) backbones would be an attractive approach to fabricate ECDs with minimal processing costs and ease of handling in the processing environment.

Water-soluble conjugated polymers (WS-CPs), which are also referred to as conjugated polyelectrolytes (CPEs), were first introduced by Wudl and Heeger et al.[19] in the synthesis of polythiophene with sulfonate derivatives, and also by our group for polypyrroles.[20,21] Since then, many water-soluble polymers with fully conjugated backbones have been synthesized and characterized. In general, these polymers are functionalized with ionic pendant groups such as sulfonate ($-SO_3^-$), carboxylate ($-CO_2^-$), phosphonate ($-PO_3^-$), and ammonium ($-NR_3^+$) to allow the organic backbones to be soluble in water.[22−25] Like most of the organic soluble CPs, WS-CPs can be synthesized via a variety of existing polymerization reactions, including oxidative methods such as electrochemical[26] and chemical oxidative polymerization,[27,28] along with transition-metal mediated methods such as Suzuki and Sonogashira polymerizations.[29−31] Of these, the ionic moiety is present on the monomer and polymerization directly affords a water-soluble polymer, or a postpolymerization functionalization route is taken where an organic soluble polymer is converted to water-soluble after polymerization and clean up. Although a large number of WS-CPs have been prepared, the investigation

Received: August 2, 2012
Accepted: September 28, 2012
Published: December 7, 2012

Scheme 1. Synthesis of Monomers

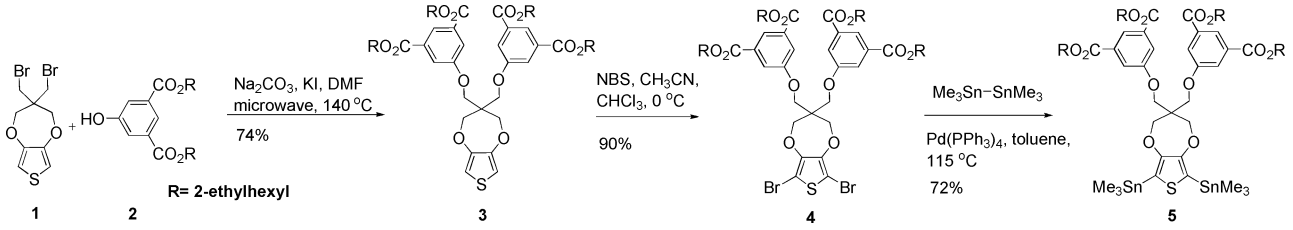

Scheme 2. Polymer Synthesis and Side-Chain Defunctionalization

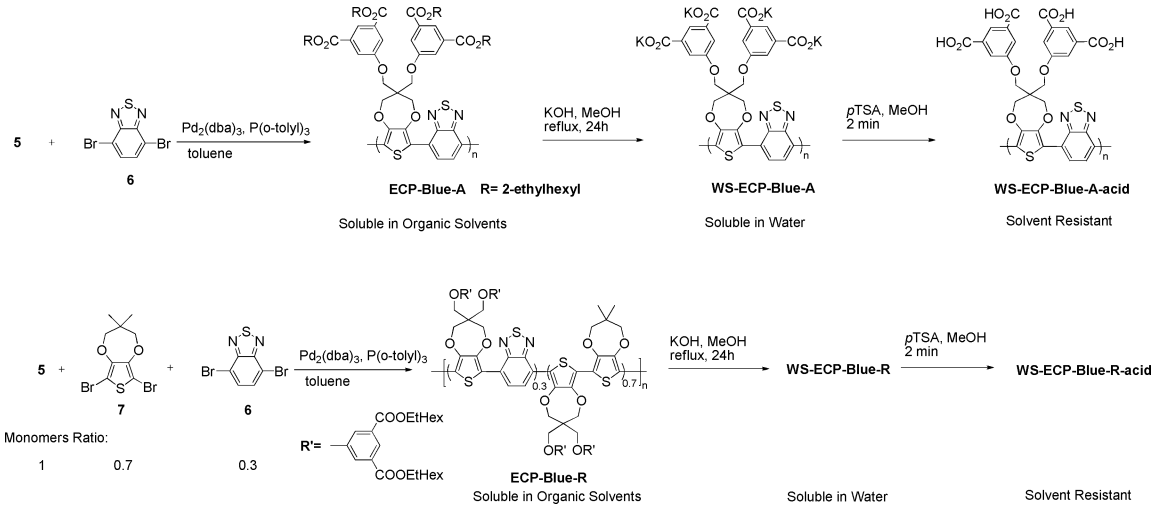

of such polymers has been mainly focused on applications in chemical and biological sensors because of their high water solubility and high optical sensitivity.[25,32,33]

In this contribution, we focus on the preparation of water processable conjugated polymers that transmit or reflect between two or more different color states upon redox activity. More specifically, we are in pursuit of polymer electrochromes with the following properties: (1) processable from an aqueous solution into solid films by existing print or spray technologies; (2) switchable from a strongly colored neutral state to a highly transmissive oxidized state for full color displays and window-type applications; and (3) exhibit short switching time (subsecond) without losing contrast when employed in electrochromic displays.

To fulfill these three requirements, several approaches have been proposed. In a previous report, Delongchamp and Hammond presented a fully functional electrochromic device, which was achieved from layer-by-layer (LbL) deposited films containing poly(aniline) (PANI) and PEDOT.[34] The device showed a reversible switch from blue-green color to yellow upon doping and undoping. Subsequently, a detailed study of alkoxy-sulfonated PEDOT polyelectrolyte was reported by our group.[35,36] Multilayer films based on the polymer and poly(allylamine hydrochloride) (PAH) were prepared by the LbL method and the electrochromic properties of the films were extensively characterized. Furthermore, a regioregular water-soluble polymer based on 3,4-propylenedioxythiophene (ProDOT) was synthesized by Kumar et al. by O-alkylation of the hydroxyl group of ProDOT−OH to prepare PProDOT-sultone.[37] Characterization of aqueous-cast films were performed in organic solvents and use of the LbL method with PAH was necessary to render films insoluble in aqueous solutions and allow for aqueous electrolyte switching. Electrochromic devices consisting of PProDOT-sultone/PAH bilayer films and an aqueous gel electrolyte (based on a sulfonic acid acrylic polymer) demonstrated switching times on the order of 100 to 50 ms for the coloration and decoloration processes, respectively. This was attributed to the rapid movement of ions in and out of the films, and is in agreement with the same observation in our group's research mentioned above.

Subsequently, our group reported the synthesis of a series of polyProDOTs bearing cleavable carboxylate ester functional groups allowing us to purify (precipitation and Soxhlet extraction) and isolate the polymers using standard procedures.[38,39] Through the use of a side-chain defunctionalization approach a PProDOT-salt homopolymer (WS-ECP-Magenta) was obtained that can be dissolved and processed in water. Upon neutralization of aqueous spray-cast thin films, the polymer acid became insoluble in both organic solvents and water. Importantly, the resulting film, which was switched in a KNO_3/water supporting electrolyte, showed only a small loss in contrast (less than 3%) on proceeding from a switching time of 0.5 to 0.25 s, as compared with a contrast loss of around 13% from a toluene-processed PProDOT-ester film switched in a LiBTI/PC electrolyte. It is worth mentioning that preparation of the organic soluble polymer ester is advantageous as it can be easily characterized (NMR, GPC et al.) in the organic form, which is not the case with conjugated polymer electrolytes. However, we found that these solubilizing groups on the ProDOT monomer were not sufficient to allow for water-soluble donor−acceptor copolymers where an unfunctionalized acceptor repeat unit is incorporated for fine-tuning of the absorption spectra.[40−44] Therefore, we sought to design a new ProDOT repeat unit with modified pendant groups that allow a higher ionic content, which can be synthesized easily and

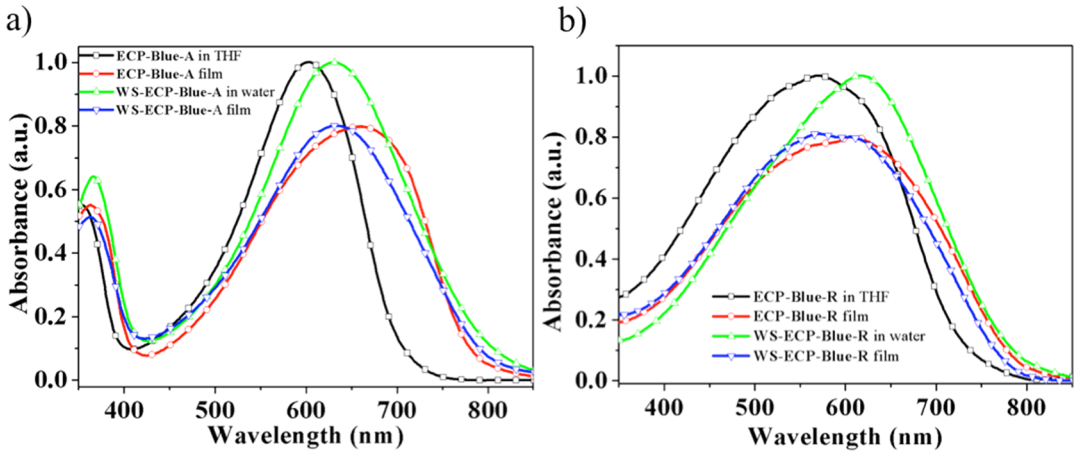

Figure 1. UV−Vis absorption spectra of (a) ECP-Blue-A and WS-ECP-Blue-A and (b) ECP-Blue-R and WS-ECP-Blue-R in dilute THF and water solution and thin films on ITO-coated glass.

provide water solubility to the resulting copolymers after defunctionalization.

In this manuscript, we report the synthesis of a new ProDOT monomer bearing four carboxylate ester groups (Scheme 1). Incorporation of the ProDOT monomer and BTD units has successfully yielded two electrochromic polymers: ECP-Blue-A (a donor−acceptor alternating copolymer) and ECP-Blue-R (a donor−acceptor random copolymer) (Scheme 2). Subsequent saponification of the ester groups afforded polymer carboxylate salts with water solubility greater than 4 mg/mL, allowing facile processing of aqueous solutions into thin films by spray-coating. The electrochromic properties of the neutralized films were evaluated and showed promising subsecond switching times.

RESULTS AND DISCUSSION

Monomer and Polymer Synthesis. Synthesis of the monomers is shown in Scheme 1. Compound **2**[45] was designed to be used as a nucleophile in a reaction with well-established dibrominated ProDOT monomer **1**[46] in order to yield a ProDOT monomer functionalized with four 2-ethylhexyl ester groups. We hypothesized that this substitution would allow solubility of the monomers and copolymers before the defunctionalization process in organic solvents, and a high ionic content after saponification to allow water solubility. Substitute of **1** with **2** proceeded efficiently under basic conditions and microwave irradiation to give compound **3** in 2 h and 74% yield after purification. The subsequent electrophilic bromination of **3** using NBS afforded compound **4** in a 90% yield. Distannyl compound **5** was subsequently synthesized by coupling **4** with hexamethyldistannane in toluene at 115 °C using $Pd(PPh_3)_4$ as the catalyst.

The alternating copolymer ECP-Blue-A (ester precursor of WS-ECP-Blue-A) was successfully prepared by Stille polymerization of distannyl compound **5** and 4,7-dibromobenzo[*c*]-[1,2,5]thiadiazole (**6**) (Scheme 2). Unexpectedly, synthesis of ECP-Blue-R by random cross-coupling of compounds **4**, **5**, and **6** in a fixed monomer feed ratio resulted in low reaction yields (less than 20%), as well as polymers with low M_n at around 7 kDa over multiple attempts. We hypothesize that steric hindrance generated from bulky side chains on the ProDOT unit prevented a high extent of reaction in this step-growth polymerization. Thus, in order to achieve high molecular weight conjugated polymers for optimal electrochromic performance, it was necessary to reduce the size of the side chains on the brominated ProDOT monomer. When compound **7**, with less bulky side chains, was utilized in the synthesis of ECP-Blue-R (Scheme 2) in place of compound **4**, the polymer M_n was increased to 14 kDa and yield increased to 85%. Both organic soluble polymers were isolated by precipitation of the reaction mixtures into methanol, followed by Soxhlet extraction with methanol and hexane. After being redissolved in chloroform, the polymers were precipitated again in methanol, and collected by filtration.

To obtain the WS-ECPs, the organic soluble ester precursors ECP-Blue-A and ECP-Blue-R were suspended separately in 1 M KOH/methanol, and the mixtures were refluxed overnight under argon. The polymer suspensions were then filtered on nylon filter membranes and washed with methanol followed by diethyl ether, and dried under vacuum. Successful saponification of the ester groups afforded WS-ECP-Blue-A and WS-ECP-Blue-R as fine powdery polymer salts, which were soluble in water at room temperature (>4 mg/mL) but insoluble in organic solvents such as toluene, THF, and chloroform. Aqueous solutions of the polymers (4 mg/mL) were spray-cast onto ITO-coated glass slides to achieve homogeneous polymer thin films with varying thicknesses. By immersing the films in a *p*TSA/MeOH solution (1 mg/mL) for 2 min, the polymers were finally converted into their acid forms, which were insoluble in water and organic solvents.

Polymer Optical Properties. Optical properties of the polymers were investigated by UV−Vis−NIR absorption spectroscopy in dilute THF solutions and as spray-cast films on ITO-coated glass. As shown in Figure 1a, ECP-Blue-A and its salt derivative WS-ECP-Blue-A exhibit a typical two-band absorption in the UV−vis spectra with an absorption minimum in the blue and bluish green region (380−550 nm). The absorption maxima of the polymers in solution as well as thin films fall into the wavelength range of 600−650 nm. Clearly, deprotection of the ester group, as well as use of a highly polar solvent, has affected the optical absorption of the chromophores in solution. The generated polymer salt WS-ECP-Blue-A demonstrates a 30 nm red shift of its long wavelength absorption peak in the aqueous solution compared with that of ECP-Blue-A in THF. Moreover, because of an improved intermolecular interaction in the solid state, the long wavelength optical transition of ECP-Blue-A thin film shows a 50 nm red shift as well as broadening of the peak compared to its

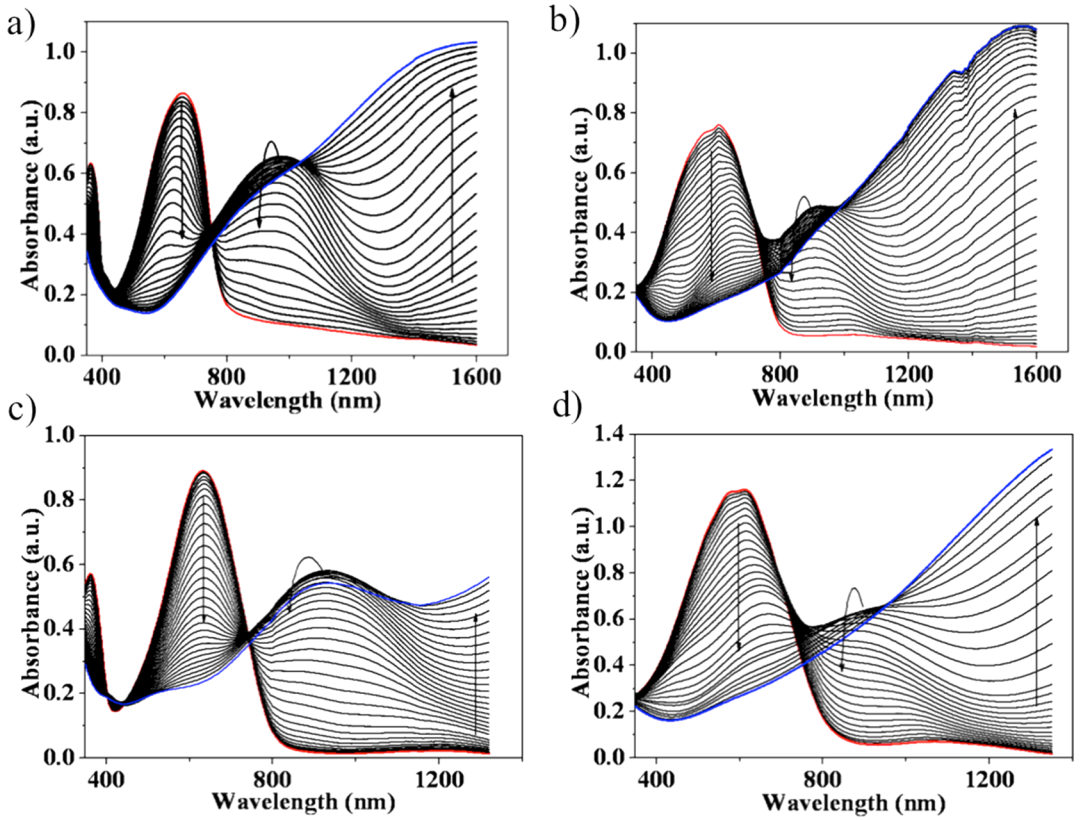

Figure 2. Spectroelectrochemistry of (a) ECP-Blue-A, (b) ECP-Blue-R, (c) WS-ECP-Blue-A-acid, and (d) WS-ECP-Blue-R-acid. The films were spray-cast onto ITO-coated glass from toluene (a and b, 3 mg mL^{-1}) or from water (c and d, 4 mg mL^{-1}). Electrochemical oxidation of the films was carried out in 0.2 M LiBTI/PC supporting electrolyte using a Ag/Ag^+ reference electrode (a and b, calibrated against Fc/Fc^+); or in 0.2 M KNO_3/water supporting electrolyte using a Ag/AgCl reference electrode (c and d). A platinum wire was used as the counter electrode. The applied potential was increased in 25 mV steps from (a) −0.25 to +0.35 V vs Fc/Fc^+, (b) −0.36 to +0.47 V vs Fc/Fc^+, (c) 0 to +0.8 V vs Ag/AgCl, and (d) −0.2 to +0.5 V vs Ag/AgCl.

solution absorption. However, in the case of water-soluble polymer WS-ECP-Blue-A, there is no dramatic change observed between the solution and film absorption. We hypothesize that this is likely due to levels of aggregation of the two polymers in solution. Given that the organic soluble polymer is likely well solvated and interaction between chains is likely minimal, as the solvent is evaporated in forming a thin film the chains aggregate efficiently. The water-soluble polymer, on the other hand, is likely in an aggregated state in aqueous solution and therefore the absorption does not shift an appreciable amount upon evaporation of the water into a thin film. As determined from the onsets of their neutral-state lower-energy optical transitions (polymer film absorption), the optical band gaps of ECP-Blue-A and WS-ECP-Blue-A are 1.56 and 1.59 eV, respectively, in good agreement with the band gaps evaluated by differential-pulse voltammetry (see the Supporting Information).

ECP-Blue-R shows a "merging" of the high- and low-energy transitions, and no obvious peak-to-peak window is observed in the visible region (Figure 1b). This effect has been noted previously for conjugated polymers with randomly incorporated repeat units as this approach has been used to produce black conjugated polymers.[12,41] However, judging by the absorption profile of ECP-Blue-R, which does not cover the entire visible region evenly, it is logical that the solution and the film of the polymer show a dark blue-black color due to lower absorptions in portions of the blue (350- 470 nm) and red (650−700 nm) regions of the spectrum. Furthermore, the broad absorption of ECP-Blue-R in THF (from 450 to 650 nm) shifts to a higher wavelength after deprotection of the ester group (see absorption spectrum of WS-ECP-Blue-R in water), which is consistent with similar observation from ECP-Blue-A. Although there is only a small λ_{max} change between WS-ECP-Blue-R water solution and its film absorption, the polymer thin film does show a broadening of the absorption in the range of 500−560 nm. However, this change in absorption is not sufficient to lead to a color change that can be observed by eye. The optical bandgaps of ECP-Blue-R and WS-ECP-Blue-R are estimated to be 1.58 and 1.60 eV, which are slightly higher than those of the corresponding ECP-Blue-A polymers.

Polymer Spectroelectrochemistry. The full spectroelectrochemical behavior of the polymers was evaluated by monitoring absorption changes of the polymer thin films upon a simultaneous change of applied external bias across the films. A film of ECP-Blue-A (λ_{max}= 655 nm, A = 0.87 au) and a film of ECP-Blue-R (λ_{max}= 609 nm, A= 0.76 au) were spray-cast onto ITO-coated glass from their 3 mg/mL toluene solutions, respectively. Electrochemical oxidation of the polymers was carried out in 0.2 M lithium bis(trifluoromethylsulfonyl)imide (LiBTI)/propylene carbonate (PC) supporting electrolyte using a Ag/Ag^+ reference electrode (calibrated against Fc/Fc^+) and a platinum wire as the counter electrode. As shown in Figure 2a and 2b, when the potential increased, the two-band absorption of ECP-Blue-A (350−400 nm and 450−700 nm) and the broad absorption of ECP-Blue-R (400−800 nm) in the visible region are depleted with appearance of the polaronic transitions[47,48] in the near-IR region from 800 to 1200 nm. As

dx.doi.org/10.1021/am3015394 | ACS Appl. Mater. Interfaces 2012, 4, 6512−6521

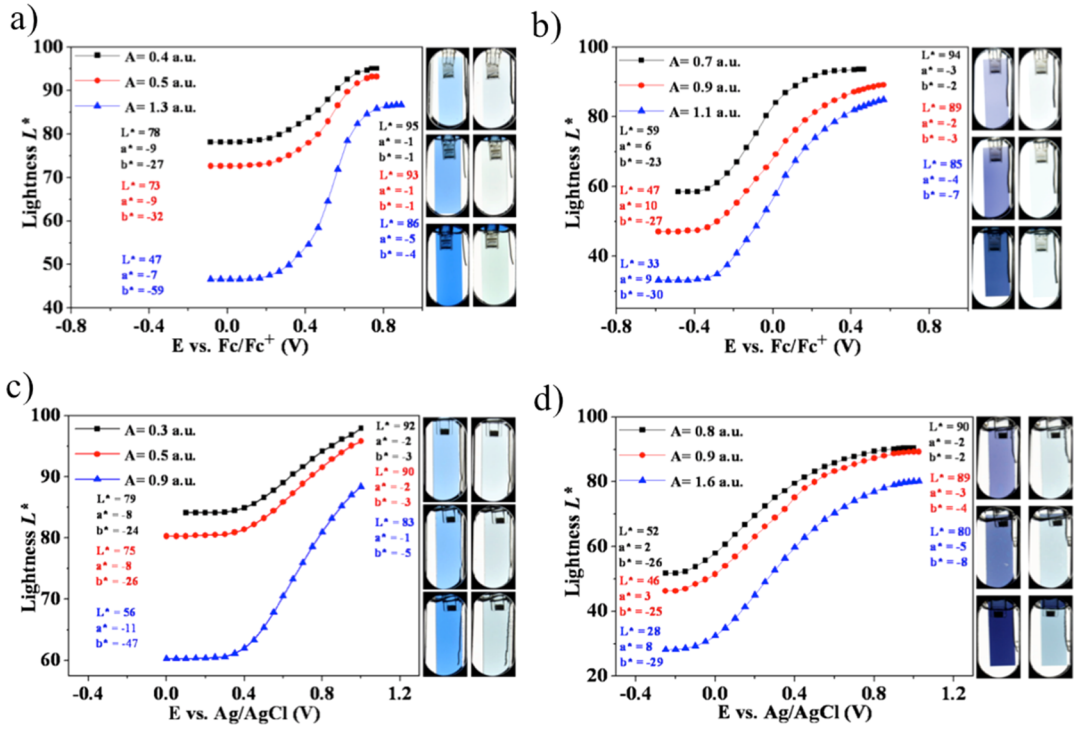

Figure 3. Lightness (L^*) as a function of applied potential for spray-coated (a) ECP-Blue-A, (b) ECP-Blue-R, (c) WS-ECP-Blue-A-acid, and (d) WS-ECP-Blue-R-acid. $L^*a^*b^*$ values of fully neutral and oxidized states are reported for the films. Photographs are of the fully neutral (left) and fully oxidized films (right).

expected, development of the polaronic transitions slows at a particular point and then decreases slightly and merges into a broader bipolaronic transition due to further increase of the oxidation potentials applied to the films. When fully oxidized, both of the polymer films show a dramatic loss of absorption in the visible region, and present a remarkably high level of transmissivity to the human eye.

The spectroelectrochemical measuremnents of WS-ECP-Blue-A-acid and WS-ECP-Blue-R-acid (Figure 2c, d) were carried out in 0.2 M aqueous KNO_3 supporting electrolyte using a Ag/AgCl reference electrode. The spray-cast polymer films were prepared from their aqueous solutions and neutralized as previously described. In the neutral state, the film absorptions of the polymer acids show good agreement with that of their salts, which means no further optical change upon treatment of the films with *p*TSA/MeOH solution. A transmittance change ($\Delta\%T$) of 46% is estimated by examining the depletion of the long wavelength absorption maximum at 630 nm for WS-ECP-Blue-A-acid, indicating a well-defined electrochromic performance. However, WS-ECP-Blue-R-acid shows a transmittance change of 51% at 555 nm, the wavelength at which the human eye has greatest sensitivity. Here, it is obvious that the thin film of WS-ECP-Blue-R-acid starts oxidizing at a lower potential (−0.2 V vs Ag/AgCl) than that of WS-ECP-Blue-A-acid (0 V vs Ag/AgCl), which is also observed in ECP-Blue-R and ECP-Blue-A (−0.36 and −0.25 V vs Fc/Fc^+, respectively). This is due to the increase in donor ratio in the random ECP-Blue-R polymer, thus raising the HOMO level.

Colorimetric Measurements. Colorimetric analysis of the polymer films with varying thickness was performed in order to evaluate color changes of the ECPs occurring on electrochemical oxidation (on the basis of the "Commission Internationale de l'Eclairage" 1976 $L^*a^*b^*$ color standards).[49,50] Before measurement, films were spray-cast and redox-cycled several times using the same conditions for each polymer, as previously discussed in the spectroelectrochemistry experiment. Figure 3 shows the determined L^* values as a function of applied voltage. This gives an indication of relative transmission of the films as they are oxidized while illuminated from behind (in essence a measure of the attenuation of light intensity as it is passing through the film) with a standard D50 simulated daytime light source. Here, in the neutral state, films of ECP-Blue-A exhibit L^* values from 47 for the thickest film (A = 1.3 au) to 78 for the thinnest film (A = 0.4 au) (Figure 3a). Moreover, a saturated blue color at all film thicknesses, which is supported by the large negative b^* values, is also observed. As expected, a small amount of green light, as indicated by the relative small negative a^* values, also passed through the polymer films because of the partial absorption missing in the range between 500 and 600 nm. By increasing the applied potentials, the polymer films begin to increase in transmission dramatically at about 0.2 V vs Fc/Fc^+. Upon full oxidation, ECP-Blue-A demonstrates L^* values ranging from 86 to 95 depending on the optical density of the thin films. In the mean time, the decreased a^* and b^* values fall into the "colorless" range. Judging by the potential shift corresponding to the lightness change, the potential window of the polymer full switch is calculated to be 0.6 V.

Compared with ECP-Blue-A, ECP-Blue-R illustrates an obvious drop of L^* value in its neutral state, which represents a deeper darkness of the sample. For example, an ECP-Blue-R film with an optical density A = 1.1 au shows a L^* value at about 33 (Figure 3b), which is lower than that of an ECP-Blue-A film with a even higher optical density (A = 1.3 au, L^* = 47). Clearly, this is due to the broad absorption nature of the polymer. However, as discussed previously, the broad absorption of ECP-Blue-R does not evenly cover the entire

dx.doi.org/10.1021/am3015394 | ACS Appl. Mater. Interfaces 2012, 4, 6512−6521

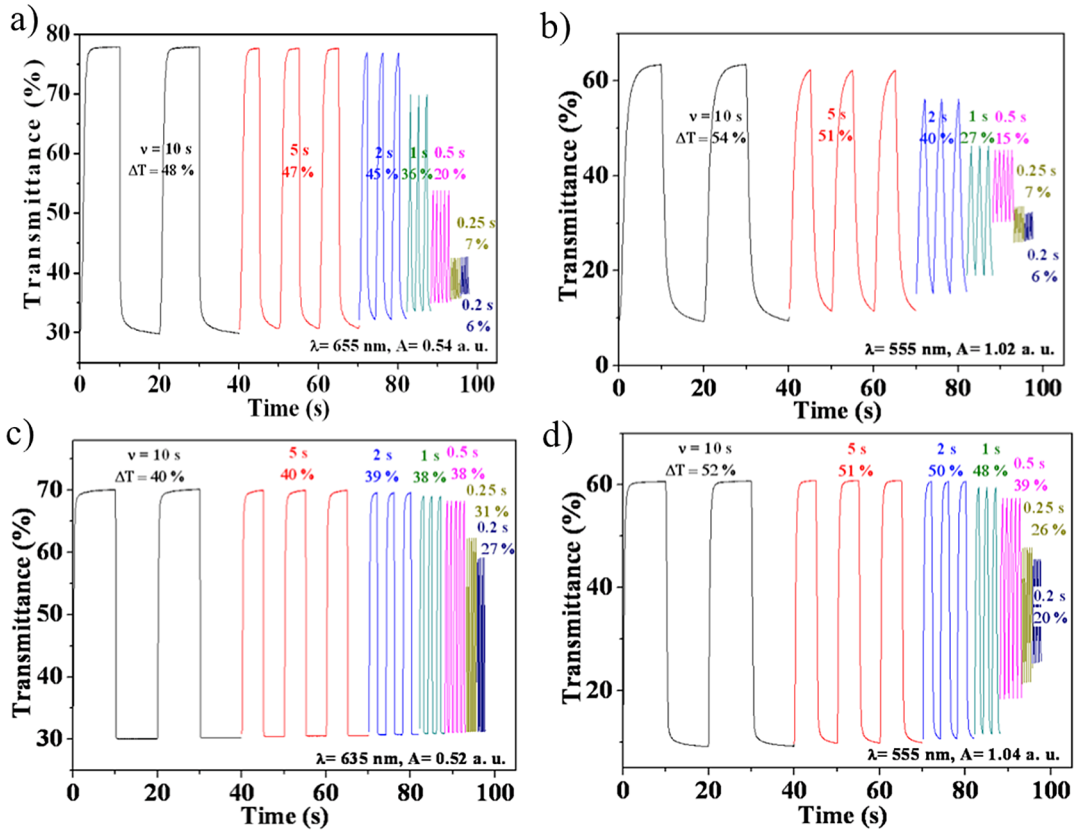

Figure 4. Square-wave potential-step chronoabsorptometry of (a) ECP-Blue-A (monitored at 655 nm, switching potential range: −0.31 to +0.74 V vs Fc/Fc^+) and (b) ECP-Blue-R (monitored at 555 nm, switching potential range: −0.49 to +0.56 V vs Fc/Fc^+) in 0.2 M LiBTI/PC electrolyte solution; (c) WS-ECP-Blue-A-acid (monitored at 635 nm, switching potential range −0.1 to +0.95 V vs Ag/AgCl) and (d) WS-ECP-Blue-R-acid (monitored at 555 nm, switching potential range −0.2 to +0.95 V vs Ag/AgCl) in 0.2 M KNO_3/water electrolyte solution. The switch times (10, 5, 2, 1, 0.5, 0.25, and 0.2 s) are indicated on the figure.

visible spectrum, and thus allows part of the red and blue light to pass through the films, as indicated by the small positive a^* values and the relatively large negative b^* values. For instance, the color of the neutral polymer film (A = 0.9 au) falls into a red-blue color region, which presents a dark blue-black color (a^* = 10, b^* = −27). When fully oxidized, the polymer film shows a highly transmissive faint blue green tint with a^* = −2 and b^* = −3.

Changing to a KNO_3/water supporting electrolyte with Ag/AgCl as the reference electrode, WS-ECP-Blue-A-acid and WS-ECP-Blue-R-acid show features in the EC performance similar to those in the corresponding polymer esters. The prominent increase of L^* values, as well as decrease in a^* and b^* values, is direct evidence of the polymers being switched into a highly transmissive state upon oxidation. It is worth mentioning that the measurements were stopped when the potential was about 1 V vs Ag/AgCl to avoid overoxidation of the polymer films and oxidation of water. Under these conditions, the experimental data was unable to show the L^* saturation of its fully oxidized state for WS-ECP-Blue-A-acid (Figure 3c). Fortunately, the polymer films still present satisfactory transmissive states as defined by the $L^*a^*b^*$ color coordinate. For example, a WS-ECP-Blue-A-acid film with an optical density A = 0.5 au shows a L^* value of 90 with a^* = −2 and b^* = −3 in its oxidized state, which are comparable to these values of an ECP-Blue-A film with the same optical density (A = 0.5 au, L^* = 93, a^*= −1 and b^*= −1, see Figure 3a). The potential window of WS-ECP-Blue-A-acid in a near full switch is 0.7 V, which is close to that of ECP-Blue-A (0.6 V). Because of the high HOMO level of WS-ECP-Blue-R-acid, which allows easier oxidation, the polymer reaches its fully oxidized state at 0.9 V vs Ag/AgCl. For a thick film (A = 1.6 au), WS-ECP-Blue-R-acid presents an intense blue-black neutral state (L^* = 28) and a faint blue transmissive state when fully oxidized (L^* = 80); a lightness change higher than 50%.

Polymer Switching Studies. To evaluate the switching rate of the polymers, the transmittance change (EC contrast, $\Delta\%T$) at a single wavelength was monitored as a function of time by applying square-wave potential steps for periods of 10, 5, 2, 1, 0.5, 0.25, and 0.2 s. The switching studies of the polymer esters and acids were carried out in 0.2 M LiBTI/PC and KNO_3/water supporting electrolytes, respectively. In Figure 4a, ECP-Blue-A shows a transmittance change as high as 48% at the longer switch time (10 s), which is only minimally reduced to 45% for the 2 s switch. Further decrease in the switch time causes a significant loss of contrast. For example, only 40% of the full contrast ($\Delta\%T$ = 20%) remains at the 0.5 s switch, and this number drops to about 12% of the full contrast ($\Delta\%T$ = 6%) at the 0.2 s switch, where the switch of the polymer can barely be detected. For an ECP-Blue-R film with an optical density of A = 1.02 au (Figure 4b), the contrast drops from 54% to 40% when the switch time is reduced from 10 to 2 s. This represents an earlier stage contrast loss, which is quite probably due to the increased thickness of the ECP-Blue-R film resulting in a slower response due to longer diffusion distances required by mobile charges and counterions.

dx.doi.org/10.1021/am3015394 | ACS Appl. Mater. Interfaces 2012, 4, 6512−6521

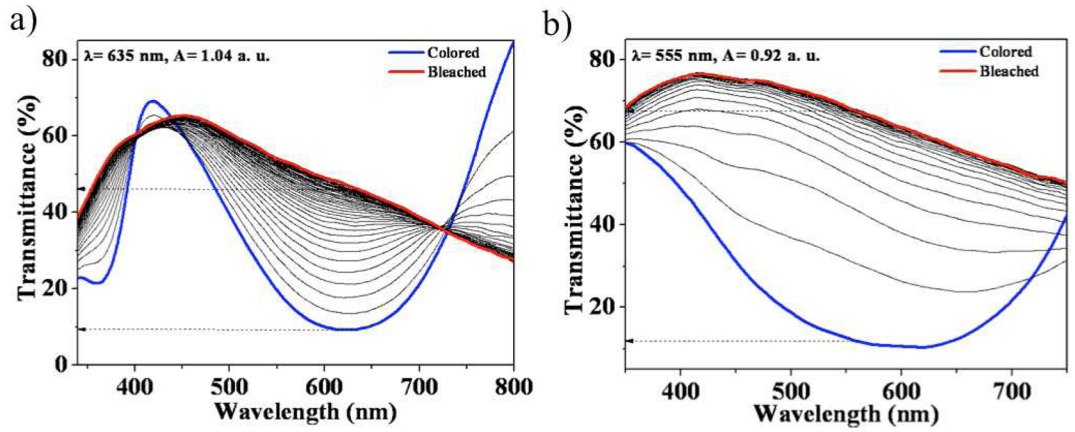

Figure 5. Rapid full spectrum measurement of (a) WS-ECP-Blue-A-acid and (b) WS-ECP-Blue-R-acid film. Switching from −0.2 V to +0.8 V vs Ag/AgCl with the full potential step in 0.2 M KNO_3/water electrolyte solution. Spectra are showed at 50 ms intervals for a total of 41 spectra in 2000 ms.

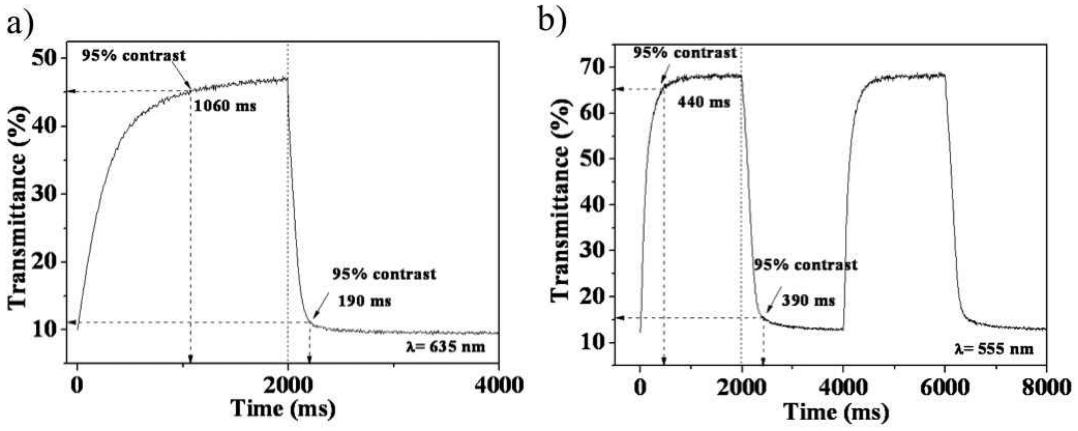

Figure 6. Time dependence of (a) WS-ECP-Blue-A-acid at 635 nm and (b) WS-ECP-Blue-R-acid at 555 nm with an applied 2 s potential square-wave from −0.2 V to +0.8 V vs Ag/AgCl in 0.2 M KNO_3/water electrolyte solution.

To compare switching performance, the polymer acid films were obtained with nearly identical thickness as their corresponding ester films (taking the optical density as representative of the thickness). As shown in Figure 4c, the WS-ECP-Blue-A-acid film, which is switched in a 0.2 M KNO_3/water electrolyte solution, exhibits a faster EC switching speed than that of ECP-Blue-A. From 10 to 0.5 s switch time, there is only a 5% loss of the full contrast observed compared with 60% for an ECP-Blue-A film with the same optical density. Unfortunately, the WS-ECP-Blue-A-acid film shows a bit lower contrast compared to its ester film even at the 10 s switch time, since the film is not fully oxidized as discussed in the Colorimetric Measurements. On the other hand, a WS-ECP-Blue-R-acid film with an optical density of A = 1.04 au (Figure 4d), has a comparable contrast (52%, 10 s switch time) as its ester film, and is still able to maintain the contrast at 48% when the switch time is reduced to 1 s. The faster switching speed is attributed to a better affinity to the electrolyte to the defunctionalized polymers, as well as the lower solution resistance of the aqueous-based electrolyte compared to that of the organic-based electrolyte.[38]

Rather than monitoring only the transmittance change at one single wavelength, fast switching polymer films of WS-ECP-Blue-A-acid and WS-ECP-Blue-R-acid were also subjected to a technique, wherein the electrochromic properties are evaluated by associating a time parameter with a full visible spectrum change during the electrochromic transition.[51] Using a spectrophotometer with a fiber-optic cable coupled to a light source and a photodiode array detector, this measurement is capable of rapid data acquisition to track the electrochromic change in the polymer films across the visible region simultaneously. It is important to note that this absorption/transmission profile is not a typical spectroelectrochemical experiment in which the electrochromic film is monitored at a steady-state (i.e., constant applied potential). Rather, it is an in situ measurement of the dynamic change in the film optical transitions. In this measurement, polymer films were stepped between the neutral and the oxidized states (−0.2 and +0.8 V vs Ag/AgCl) using a 2 s switch time, and the optical spectra were captured every 6 ms during the electrochromic transition period. The selected transmittance spectra in Figure 5 are shown at intervals of 50 ms for clarity (A total of 41 spectra are abstracted from nearly 320 spectra in a 2 s switch.).

For WS-ECP-Blue-A-acid, the polymer film in the colored neutral state shows a low transmittance of 10% at λ_{max} (635 nm). Upon applying a positive potential (+0.8 V vs Ag/AgCl) to the polymer film, the transmittance steadily increases to a higher level (Figure 5a). When the bleached state is reached, the film shows a transmittance of 46% with a transmittance contrast of 36% ($\Delta\%T$) at 635 nm. Although the polymer

shows a dual-band absorption, the high energy band with λ_{max} at 370 nm will not be discussed in this case, since the human eye is not sensitive at that region. Moreover, the polymer film of WS-ECP-Blue-R-acid demonstrates a transmittance of 12% in the neutral state and 68% in the fully bleached state at 555 nm with a transmittance contrast of 56% (Figure 5b).

Another aspect in this methodology is that an estimate of the switching speed profile can be roughly observed in the absorption/transmission spectra, because each spectrum shown has a 50 ms time separation in Figure 5a and 5b. This provides a time-stamp in the whole spectra. In the case of WS-ECP-Blue-A-acid, the transmission increase in the long wavelength region (500−700 nm) is relatively steady and slow, and the first 20 spectra can be clearly observed in the figure. However, the WS-ECP-Blue-R-acid shows a more pronounced transmission increase, so that the spectra after the first 10 transitions are compressed at a transmission level close to the fully bleached state, indicating a faster switching speed compared to the alternating blue polymer.

To quantitatively evaluate how fast the polymers are switched, the transmittance values at a single wavelength were extracted from the collected data and plotted as a function of their acquisition times. Figure 6a shows the results for WS-ECP-Blue-A-acid at 635 nm. Judging by the transmittance profile, which is still increasing after 2 s, the polymer film is unable to reach a fully transmissive oxidized state in this time frame using a potential of +0.8 V vs Ag/AgCl. Although the low potential will protect the polymer film from being overoxidized and oxidation of the solvent, it could lower the switching speed because of insufficient driving force for ion motion, and lower the contrast as well since the polymers are not fully oxidized. In this case, 95% of the full transmittance contrast ($t_{95\%}$) for the bleaching process is achieved after 1060 ms (from transmittance of T = 9.6% to T = 45.0%), whereas the neutralization process is achieved in 190 ms (from T = 46.9% to T = 11.5%).

On the other hand, WS-ECP-Blue-R-acid presents a fully bleached state in the 2 s time frame (Figure 6b). This is due to the polymer's low oxidation potential (high HOMO level), which results in a large potential difference compared to +0.8 V vs Ag/AgCl, and thus a stronger driving force for ion motion. A $t_{95\%}$ (from T = 12.9% to T = 65.4%) of 440 ms is observed for the bleaching process, which is faster than that of WS-ECP-Blue-A-acid ($t_{95\%}$ = 1060 ms). However, a slightly slower neutralization process is observed with $t_{95\%}$ of 390 ms (from T = 68.2% to T = 15.7%).

CONCLUSIONS

We have demonstrated the synthesis of two new donor−acceptor ECPs by Stille polymerization: a blue-to-transmissive conjugated polymer (ECP-Blue-A) and a dark blue-black-to-transmissive conjugated polymer (ECP-Blue-R). These copolymers were functionalized with side chains containing four ester groups per donor moiety, allowing organic solubility in the ester form, and water solubility in their carboxylate salt form even without side chain functionalization of the acceptor. Importantly, the polymer carboxylate salts display water solubility greater than 4 mg/mL, which allows facile processing from aqueous solutions to thin films by spray-casting onto ITO coated substrates. Upon subsequent neutralization of the carboxylate salts to carboxylic acids, the resulting polymer acid films are solvent resistant and can be electrochemically switched between their colored states and a transmissive state in an aqueous KNO_3 electrolyte solution, and show a dramatic improvement in the EC switching speed performance compared with their ester derivatives at the subsecond switching time scale. The results of the electrochromic properties study indicate that these water-soluble electrochromic conjugated polymers are promising candidates for rapid switching electrochromic devices.

EXPERIMENTAL SECTION

Instrumentation. ^{1}H NMR (300 MHz) and ^{13}C NMR (75 MHz) spectra were recorded on a Mercury 300 MHz spectrometer using deuterated chloroform as solvent and tetramethylsilane as internal reference. Elemental analyses were performed by the CHN elemental analysis service in the Chemistry Department of the University of Florida and the Robertson Microlit Laboratories, Inc., Atlantic Microlab, Inc. High resolution mass spectrometry was performed by the spectroscopic services in the Chemistry Department of the University of Florida with a Finnigan MAT 95Q Hybrid Sector or a Bruker APEX II FTICR or Agilent 6210 TOF. Gel permeation chromatography (GPC) was performed using a Waters Associates GPCV2000 liquid chromatography system with its internal differential refractive index detector (DRI) at 40 °C, using two Waters Styragel HR-5E columns (10 μm PD, 7.8 mm i.d., 300 mm length) with HPLC grade THF as the mobile phase at a flow rate of 1.0 mL min^{-1}. Injections were made at 0.05 - 0.07% w/v sample concentration using a 220.5 μL injection volume. Retention times were calibrated against narrow molecular weight polystyrene standards (Polymer Laboratories; Amherst, MA). Analytical HPLC was done on a Hitachi EZ chrome system, using a Lachrom ultra 4.6 mm × 150 mm C18 (TMS end-capped, 5 M particle size) column, using 30% acetonitrile 70% THF at 2 mL/min as eluent and detected at 265 nm. Preparative HPLC was done using the Lachrom ultra 21.2 mm × 250 mm C18 (TMS end-capped, 10 M particle size) column at using 30% acetonitrile 70% THF at 8 mL/min as eluent and detected at 265 nm. Electrochemistry was performed using a three-electrode cell with a platinum wire or a platinum flag as the counter electrode, a Ag/Ag$^+$ (used for nonaqueous solutions) or Ag/AgCl (used with aqueous solutions) as the reference electrode, and a platinum button or ITO-coated glass slide (7 × 50 × 0.7 mm^3, 20 Ω/sq) as the working electrode. The ITO electrodes were purchased from Delta Technologies, Ltd. All potentials were reported vs Fc/Fc$^+$ or vs Ag/AgCl. An EG&G Princeton Applied Research model 273 potentiostat was used under the control of CorrWare II software from Scribner and Associates. For all optical measurements, the spectra were corrected with respect to a reference that included the cuvette, ITO/glass electrode, and electrolyte solution. Absorption spectra including in situ spectroelectrochemistry studies were performed using a Varian Cary 500 Scan UV−vis/NIR spectrophotometer. In situ spectroscopic analysis was also handled by an Ocean Optics USB2000+ spectrophotometer detector and associated Ocean Optics DH-2000-BAL fiber-optic light source. The detector was placed, along with cuvette holders, in an enclosure designed to eliminate extraneous light. In situ colorimetric measurements were performed using a Minolta CS100 Colorimeter in transmission mode with a GraphicLite LiteGuard II standard D50 light source. The light source and the sample to be measured were placed in a color viewing booth. The interior of the light booth is coated with a standard gray neutral 8 (GTI Graphic Technology, Inc.) matte latex enamel (equivalent to Munsell N8) to allow for accurate assessment of color of the sample during measurement. Photography was performed in the same light booth using a Nikon D90 at an exposure time of 1/80 s, f-stop of f/5.3, ISO sensitivity of 200, and focal length of 18−105 mm. The photograph file-type was JPEG and the files were cropped to only the polymer film to exclude extraneous background using Adobe Photoshop. No additional alterations to the photography files were performed.

Materials. All chemical reagents and dehydrated solvents were commercially available and used without further purification unless otherwise noted. All reactions were carried out with oven-dried glassware and dry solvents in Argon atmosphere unless otherwise

stated. For column chromatography, Whatman Purasil silica gel (230–400 Mesh, pore diameter 6 nm) was used. 4,7-Dibromobenzo[*c*]-[1,2,5]thiadiazole (**6**)[52] and 6,8-dibromo-3,3-dimethyl-3,4-dihydro-2H-thieno[3,4-b][1,4]dioxepine (**7**)[45] were prepared as previously described.

*Bis(2-ethylhexyl) 5-Hydroxyisophthalate (**2**).* To a stirred suspension of 5-hydroxy-isophthalic acid (30 g, 165 mmol) and 2-ethylhexan-1-ol (51.5 g, 395 mmol) in 250 mL of toluene was added concentrated H_2SO_4 (5 drops), and the reaction mixture was refluxed with a Dean–Stark apparatus for 48 h. After removal of unreacted 5-hydroxy-isophthalic acid by filtration, the residue was washed with water three times and dried over anhydrous $MgSO_4$. The solvent was evaporated and the residue was purified by flash chromatography using 8:1:1 hexane: ethyl acetate: acetone to give compound 2 as a yellow oil (50 g, 75%). ^{1}H NMR ($CDCl_3$): δ 8.22 (t, 1H, J = 1.2 Hz), δ 7.85 (d, 2H, J = 1.2 Hz), δ 7.06 (br, 1H), δ 4.27 (d, 4H, J = 5.7 Hz), δ 1.72 (m, 2H), δ 1.50–1.31 (m, 16H), δ 0.96–0.87 (m, 12H). ^{13}C NMR ($CDCl_3$): δ 166.52, 156.82, 132.32, 122.75, 121.23, 68.17, 39.10, 30.73, 29.18, 24.17, 23.16, 14.23, 11.28. HRMS (ESI–FTICR): m/z calcd for $C_{24}H_{38}NaO_5$ ($M+Na^+$) 429.2611 found 429.2618. Anal. Calcd for $C_{24}H_{38}O_5$: C 70.90, H 9.42, found C 70.53, H 9.78.

*Tetrakis(2-ethylhexyl) 5,5′-(3,4-Dihydro-2H-thieno[3,4-b][1,4]-dioxepine-3,3-diyl)bis(methylene)bis(oxy)diisophthalate (**3**).* Compound **1** (5 g, 14.6 mmol), compound **2** (17.8 g, 43.8 mmol), K_2CO_3 (12.1 g, 87.7 mmol), KI (0.97 g, 5.9 mmol), and DMF (60 mL) were added to a 100 mL round-bottom flask. The solution was heated by microwave irradiation (200 W) at 140 °C for 1 h. After removal of the solids by filtration, the reaction mixture was diluted with methylene chloride (50 mL) and washed with water. The organic phase was dried over $MgSO_4$ and the solvent was removed. The crude product was purified by column chromatography on silica gel (hexane: ethyl acetate, 9:1) to yield the desired product as a yellow oil (10.8 g, 74%). ^{1}H NMR ($CDCl_3$): δ 8.26 (t, 2H, J = 1.2 Hz), δ 7.75 (d, 4H, J = 1.5 Hz), δ 6.52 (s, 2H), δ 4.31 (s, 4H), δ 4.30 (s, 4H), δ 4.24 (d, 8H, J = 6.0 Hz), δ 1.72 (m, 4H), δ 1.48–1.26 (m, 32H), δ 0.97–0.86 (m, 24H). ^{13}C NMR ($CDCl_3$): δ 165.85, 158.75, 149.34, 132.50, 123.54, 119.82, 105.91, 72.88, 68.05, 67.12, 47.61, 39.08, 30.74, 29.18, 24.18, 23.16, 14.26, 11.27. HRMS (ESI–FTICR): m/z calcd for $C_{57}H_{85}O_{12}S$ ($M+H^+$) 993.5756 found 993.5740. Anal. Calcd for $C_{57}H_{84}O_{12}S$: C, 68.92; H, 8.52. Found: C, 68.68; H, 8.74.

*Tetrakis(2-Ethylhexyl) 5,5′-(6,8-dibromo-3,4-dihydro-2H-thieno-[3,4-b][1,4]dioxepine-3,3-diyl)bis(methylene)bis(oxy)diisophthalate (**4**).* A solution of NBS (1.1 g, 6.3 mmol, in 15 mL acetonitrile) was added slowly to a solution of compound **3** (3.0 g, 3.0 mmol) in chloroform (15.0 mL) 0 °C. The mixture was stirred at the same temperature for 2 h before allowing it to warm to room temperature. After stirring at room temperature for overnight, the solution was diluted with methylene chloride (50 mL) and the organic phase was washed with water and dried over anhydrous $MgSO_4$. The solvent was evaporated and the residue was purified by column chromatography on silica gel (hexane: ethyl acetate, 9:1) to yield the desired product as a light yellow oil (3.1 g, 90%). ^{1}H NMR ($CDCl_3$): δ 8.27 (t, 2H, J = 1.2 Hz), δ 7.74 (d, 4H, J = 1.2 Hz), δ 4.38–4.25 (m, 16H), δ 1.72 (m, 4H), δ 1.51–1.26 (m, 32H), δ 0.97–0.85 (m, 24H). ^{13}C NMR ($CDCl_3$): δ 165.78, 158.53, 146.67, 132.54, 123.67, 119.75, 91.88, 73.25, 68.07, 66.80, 47.75, 39.07, 30.72, 29.17, 24.17, 23.16, 14.26, 11.27. HRMS (ESI–FTICR): m/z calcd for $C_{57}H_{83}Br_2O_{12}S$ ($M+H^+$) 1151.3955 found 1151.3917. Anal. Calcd for $C_{57}H_{82}Br_2O_{12}S$: C 59.47, H 7.18, found C 59.68, H 7.49.

*Tetrakis(2-Ethylhexyl) 5,5′-(6,8-bis(trimethylstannyl)-3,4-dihydro-2H-thieno[3,4-b][1,4]dioxepine-3,3-diyl)bis(methylene)bis(oxy)-diisophthalate (**5**).* A solution of compound **4** (5 g, 4.3 mmol), hexamethylditin (4.3 g, 13.1 mmol), and $Pd(PPh_3)_4$ (1 g, 0.9 mmol) in toluene (50 mL) was degassed three times by successive freeze–pump–thaw cycles and then heated to 115 °C for 3 h, during which time TLC analysis indicated completion of the reaction. The reaction mixture was then cooled to room temperature and water was added. After extraction with methylene chloride, the organic phase was dried with anhydrous $MgSO_4$ and solvent was removed under vacuum. The crude compound was purified by reverse-phase HPLC to give 4.1 g of a colorless oil (72%). ^{1}H NMR ($CDCl_3$): δ 8.27 (t, 2H, J = 1.2 Hz), δ 7.77 (d, 4H, J = 1.2 Hz), δ 4.33–4.23 (m, 16H), δ 1.75 (m, 4H), δ 1.50–1.35 (m, 32H), δ 0.98–0.88 (m, 24H), δ 0.35 (s, 18H). ^{13}C NMR ($CDCl_3$): δ 165.86, 158.84, 156.28, 132.42, 124.10, 123.35, 119.79, 72.94, 67.98, 67.42, 47.34, 39.05, 30.71, 29.15, 24.16, 23.12, 14.22, 11.25, −8.35. Anal. Calcd for $C_{63}H_{100}O_{12}SSn_2$: C, 57.37; H, 7.64. Found: C, 57.65; H, 7.73.

Polymer ECP-Blue-A. A solution of compound **5** (0.9 g, 0.68 mmol), compound **8** (0.201 g, 0.68 mmol), tris(dibenzylideneacetone)dipalladium (0) (13.8 mg, 0.015 mmol), and tri(*o*-tolyl)-phosphine (18.3 mg, 0.06 mmol) in toluene (20 mL) were charged in a 50 mL Schlenk tube and degassed three times by successive freeze–pump–thaw cycles, then heated at 115 °C for 36 h in an oil bath. The solution was then precipitated into methanol (400 mL). The precipitate was filtered through a cellulose thimble and purified via Soxhlet extraction for 24 h with methanol and then 48 h with hexane. The polymer was extracted with chloroform, concentrated by evaporation, and then precipitated into methanol again (400 mL). The collected polymer was a blue solid (0.7 g, 91%). ^{1}H NMR (300 MHz, $CDCl_3$) δ 8.41 (s, 2H), 8.27 (s, 2H), 7.81 (d, 4H, J = 0.9 Hz), 4.67 (s, 4H), 4.50 (s, 4H), 4.30–4.20 (m, 8H), 1.74–1.29 (m, 36H), δ 0.95–0.85 (m, 24H). GPC analysis: M_n = 25.8 kDa, M_w = 38.5 kDa, PDI = 1.5. Anal. Calcd. for $C_{63}H_{84}N_2O_{12}S_2$: C 67.23, H 7.52, N 2.49, found C 66.94, H 7.64, N 2.42.

ECP-Blue-R. Compound **5** (0.9 g, 0.682 mmol), compound **7** (0.163 g, 0.478 mmol), compound **8** (0.060 g, 0.205 mmol), tris-(dibenzylideneacetone)dipalladium (0) (13.8 mg, 0.015 mmol), and tri(*o*-tolyl)phosphine (18.3 mg, 0.06 mmol), and toluene (20 mL) were charged in a 50 mL Schlenk tube and the above procedure was followed. The collected polymer was a black solid (0.66 g, 84%). ^{1}H NMR (300 MHz, $CDCl_3$) δ 8.25 (m, 13H), 7.79 (s, 20H), 4.48–4.21 (m, 80H), 4.50 (s, 4H), 3.85 (s, 14H), 1.69–1.11 (m, 180H), δ 0.95–0.85 (m, 141H). GPC analysis: M_n = 13.9 kDa, M_w = 23.3 kDa, PDI = 1.7. Anal. Calcd. for $C_{651}H_{896}N_6O_{134}S_{20}$: C, 67.46; H, 7.79; N, 0.73. Found: C, 67.11; H, 7.89; N, 0.68.

WS-ECP-Blue-A. A solution of 1 M KOH in methanol (50 mL) was refluxed and simultaneously sparged with argon for two hours, and ECP-Blue-A (360 mg) was added as a solid. This suspension was refluxed for 24 h, during which time the polymer dispersed into fine particles. The suspension was filtered on a nylon filter membrane and washed with 100 mL of methanol followed by 100 mL of diethyl ether, and dried under a vacuum to yield 260 mg of a dark solid (90%).

WS-ECP-Blue-R. The same reaction and purification procedure as described for WS-ECP-Blue-A was followed, except ECP-Blue-R (395 mg) was used. Polymer WS-ECP-Blue-R was obtained as a dark black powder (300 mg, 92%).

■ ASSOCIATED CONTENT

Ⓢ Supporting Information

Additional GPC and elemental analysis results, electrochemical data including DPV of polymers. This material is available free of charge via the Internet at http://pubs.acs.org.

■ AUTHOR INFORMATION

Corresponding Author

*E-mail: reynolds@chemistry.gatech.edu.

Notes

The authors declare no competing financial interest.

■ ACKNOWLEDGMENTS

We gratefully acknowledge funding of this work by the AFOSR (FA9550-09-1-0320), the ONR (N00014-08-1-0928), and BASF.

■ REFERENCES

(1) Skotheim, T. A.; Reynolds, J. R. *Handbook of Conducting Polymers*; CRC Press: London, 2007.

(2) Burroughes, J. H.; Bradley, D. D. C.; Brown, A. R.; Marks, R. N.; Mackay, K.; Friend, R. H.; Burn, P. L.; Holmes, A. B. *Nature* **1990**, *347*, 539.
(3) Braun, D.; Heeger, A. J. *Appl. Phys. Lett.* **1991**, *58*, 1982.
(4) Bernius, M. T.; Inbasekaran, M.; O'Brien, J.; Wu, W. *Adv. Mater.* **2000**, *12*, 1737.
(5) Yu, G.; Gao, J.; Hummelen, J. C.; Wudl, F.; Heeger, A. J. *Science* **1995**, *270*, 1789.
(6) Scharber, M. C.; Mühlbacher, D.; Koppe, M.; Denk, P.; Waldauf, C.; Heeger, A. J.; Brabec, C. J. *Adv. Mater.* **2006**, *18*, 789.
(7) Son, H. J.; Wang, W.; Xu, T.; Liang, Y.; Wu, Y.; Li, G.; Yu, L. *J. Am. Chem. Soc.* **2011**, *133*, 1885.
(8) Tsao, H. N.; Cho, D.; J. Andreasen, W.; Rouhanipour, A.; Breiby, D. W.; Pisula, W.; Müllen, K. *Adv. Mater.* **2009**, *21*, 209.
(9) Sonar, P.; Singh, S. P.; Li, Y.; Soh, M. S.; Dodabalapur, A. *Adv. Mater.* **2010**, *22*, 5409.
(10) Dyer, A. L.; Reynolds, J. R. In *Handbook of Conducting Polymer*, 3rd ed.; Skotheim, T., Reynolds, J. R., Eds.; CRC Press: Boca Raton, FL, 2007; Vol. *1*, Chapter 20.
(11) Beaujuge, P. M.; Reynolds, J. R. *Chem. Rev.* **2010**, *110*, 268.
(12) Shi, P.; Amb, C. M.; Knott, E. P.; Thompson, E. J.; Liu, D. Y.; Mei, J.; Dyer, A. L.; Reynolds, J. R. *Adv. Mater.* **2010**, *22*, 4949.
(13) Balan, A.; Gunbas, G.; Durmus, A.; Toppare, L. *Chem. Mater.* **2008**, *20*, 7510.
(14) Heywang, G.; Jonas, F. *Adv. Mater.* **1992**, *4*, 116.
(15) Groenendaal, L. B.; Jonas, F.; Freitag, D.; Pielartzik, H.; Reynolds, J. R. *Adv. Mater.* **2000**, *12*, 481.
(16) Gustafsson, J. C.; Liedberg, B.; Inganäs, O. *Solid State Ionics* **1994**, *69*, 145.
(17) Heuer, H. W.; Wehrmann, R.; Kirchmeyer, S. *Adv. Funct. Mater.* **2002**, *12*, 89.
(18) Welsh, D. M.; Kumar, A.; Meijer, E. W.; Reynolds, J. R. *Adv. Mater.* **1999**, *11*, 1379.
(19) Patil, O.; Ikenoue, Y.; Wudl, F.; Heeger, A. J. *J. Am. Chem. Soc.* **1987**, *109*, 1858.
(20) Sundaresan, N. S.; Basak, S.; Pomerantz, M.; Reynolds, J. R. *J. Chem. Soc., Chem. Commun.* **1987**, 621.
(21) Reynolds, J. R.; Sundaresan, N. S.; Pomerantz, M.; Basak, S.; Baker, C. K. *J. Electroanal. Chem. Interfacial Electrochem.* **1988**, *250*, 355.
(22) Hoven, C. V.; Garcia, A.; Bazan, G. C.; Nguyen, T.-Q. *Adv. Mater.* **2008**, *20*, 3793.
(23) Huang, F.; Wu, H.; Cao, Y. *Chem. Soc. Rev.* **2010**, *39*, 2500.
(24) Zhu, C.; Liu, L.; Yang, Q.; Lv, F.; Wang, S. *Chem. Rev.* **2012**, *112*, 4687.
(25) Jiang, H.; Taranekar, P.; Reynolds, J. R.; Schanze, K. S. *Angew. Chem., Int. Ed.* **2009**, *48*, 4300.
(26) Krishnamoorthy, K.; Kanungo, M.; Ambade, A. V.; Contractor, A. Q.; Kumar, A. *Synth. Met.* **2002**, *125*, 441.
(27) Zotti, G.; Zecchin, S.; Schiavon, G.; Groenendaal, L. B. *Macromol. Chem. Phys.* **2002**, *203*, 1958.
(28) Ho, H. A.; Boissinot, M.; Bergeron, M. G.; Corbeil, G.; Doré, K.; Boudreau, D.; Leclerc, M. *Angew. Chem., Int. Ed.* **2002**, *41*, 1548.
(29) Liu, B.; Bazan, G. C. *J. Am. Chem. Soc.* **2004**, *126*, 1942.
(30) McQuade, D. T.; Hegedus, A. H.; Swager, T. M. *J. Am. Chem. Soc.* **2000**, *122*, 12389.
(31) Brookins, R. N.; Schanze, K. S.; Reynolds, J. R. *Macromolecules* **2007**, *40*, 3524.
(32) Thomas, S. W., III; Joly, G. D.; Swager, T. M. *Chem. Rev.* **2007**, *107*, 1339.
(33) Qin, C.; Wong, W.-H.; Wang, L. *Macromolecules* **2011**, *44*, 483.
(34) DeLongchamp, D.; Hammond, P. T. *Adv. Mater.* **2001**, *13*, 1455.
(35) Culter, C. A.; Bouguettaya, M.; Reynolds, J. R. *Adv. Mater.* **2002**, *14*, 684.
(36) Cutler, C. A.; Bouguettaya, M.; Kang, T. S.; Reynolds, J. R. *Macromolecules* **2005**, *38*, 3068.
(37) Jain, V.; Sahoo, R.; Mishra, S. P.; Sinha, J.; Montazami, R.; Yochum, H. M.; Heflin, J. R.; Kumar, A. *Macromolecules* **2009**, *42*, 135.
(38) Reeves, B. D.; Unur, E.; Ananthakrishnan, N.; Reynolds, J. R. *Macromolecules* **2007**, *40*, 5344.
(39) Beaujuge, P. M.; Amb, C. M.; Reynolds, J. R. *Adv. Mater.* **2010**, *22*, 5383.
(40) Amb, C. M.; Dyer, A. L.; Reynolds, J. R. *Chem. Mater.* **2011**, *23*, 397.
(41) Beaujuge, P. M.; Ellinger, S.; Reynolds, J. R. *Nat. Mater.* **2008**, *7*, 795.
(42) Amb, C. M.; Beaujuge, P. M.; Reynolds, J. R. *Adv. Mater.* **2009**, *22*, 724.
(43) Durmus, A.; Gunbas, G. E.; Camurlu, P.; Toppare, L. *Chem. Commun.* **2007**, 3246.
(44) Wu, C.-G.; Lu, M.-I.; Chang, S.-J.; Wei, C.-S. *Adv. Funct. Mater.* **2007**, *17*, 1063.
(45) Inouye, M.; Fujimoto, K.; Furusyo, M.; Nakazumi, H. *J. Am. Chem. Soc.* **1999**, *121*, 1452.
(46) Reeves, B. D.; Grenier, C. R. G.; Argun, A. A.; Cirpan, A.; McCarley, T. D.; Reynolds, J. R. *Macromolecules* **2004**, *37*, 7559.
(47) Bredas, J. L.; Chance, R. R.; Silbey, R. *Phys. Rev. B* **1982**, *26*, 5843.
(48) Bredas, J. L.; Scott, J. C.; Yakushi, K.; Street, G. B. *Phys. Rev. B* **1984**, *30*, 1023.
(49) Thompson, B. C.; Schottland, P.; Zong, K.; Reynolds, J. R. *Chem. Mater.* **2000**, *12*, 1563.
(50) Berns, R. S. *Billmeyer and Saltzman's Principles of Color Technology*, 3rd ed.; John Wiley & Sons: New York, 2000.
(51) Liu, D. Y.; Chilton, A. D.; Shi, P.; Craig, M. R.; Miles, S. D.; Dyer, A. L.; Ballarotto, V. W.; Reynolds, J. R. *Adv. Funct. Mater.* **2011**, *21*, 4535.
(52) DaSilveira Neto, B. A.; Lopes, A. S. A.; Ebeling, G. R.; Goncalves, S.; Costa, V. E. U.; Quina, F. H.; Dupont, J. *Tetrahedron* **2005**, *61*, 10975.